

Article

Analyzing Temporal Trends of Urban Evaporation Using Generalized Additive Models

Basem Aljoumani ^{1,*}, Jose A. Sanchez-Espigares ², Björn Kluge ³, Gerd Wessolek ⁴ and Birgit Kleinschmit ¹

¹ Geoinformation in Environmental Planning Lab, Department of Landscape Architecture and Environmental Planning, Technische Universität Berlin, 10587 Berlin, Germany; birgit.kleinschmit@tu-berlin.de

² Department of Statistical and Operational Research, Universitat Politècnica de Catalunya (UPC), Jordi Girona, 31, 08034 Barcelona, Spain; josep.a.sanchez@upc.edu

³ Department of Ecology, Ecohydrology and Landscape Evaluation, Technische Universität Berlin, 10587 Berlin, Germany; bjoern.kluge@tu-berlin.de

⁴ Department of Ecology, Soil Conservation, Technische Universität Berlin, 10587 Berlin, Germany; gerd.wessolek@tu-berlin.de

* Correspondence: basem.aljoumani@tu-berlin.de

Abstract: This study aimed to gain new insights into urban hydrological balance (in particular, the evaporation from paved surfaces). Hourly evaporation data were obtained simultaneously from two high-resolution weighable lysimeters. These lysimeters are covered in two pavement sealing types commonly used for sidewalks in Berlin, namely cobble-stones and concrete slabs. A paired experiment in field conditions is designed to determine the mechanism by which these two types of soil sealing affect the evaporation rate under the same climatic conditions. A generalized additive model (GAM) is applied to explain how the climatic conditions interact with soil sealing and to evaluate the variation of evaporation rate according to pavement type. Moreover, taking the advantage of the fact that the experimental design is paired, the study fits a new GAM where the response variable is the difference between the evaporation rate from the two lysimeters and its explanatory variables are the climatic conditions. As a result, under the same climatic conditions, cobble-stones are more prone to increasing the evaporation rate than concrete slabs when the precipitation accumulated over 10 h, solar radiation, and wind speed increases. On the other hand, concrete slabs are more inclined to increase the evaporation rate than cobblestones when the relative humidity increases. GAM represents a robust modeling approach for comparing different sealing types in order to understand how they alter the hydrological balance.

Keywords: urban evaporation; urban lysimeter; generalized additive models (GAMs); time series analysis; pavement urban hydrological balance



Citation: Aljoumani, B.; Sanchez-Espigares, J.A.; Kluge, B.; Wessolek, G.; Kleinschmit, B. Analyzing Temporal Trends of Urban Evaporation Using Generalized Additive Models. *Land* **2022**, *11*, 508. <https://doi.org/10.3390/land11040508>

Academic Editor: Nir Krakauer

Received: 14 February 2022

Accepted: 29 March 2022

Published: 31 March 2022

Publisher's Note: MDPI stays neutral with regard to jurisdictional claims in published maps and institutional affiliations.



Copyright: © 2022 by the authors. Licensee MDPI, Basel, Switzerland. This article is an open access article distributed under the terms and conditions of the Creative Commons Attribution (CC BY) license (<https://creativecommons.org/licenses/by/4.0/>).

1. Introduction

Paved surfaces are a necessary infrastructure of cities, which are traditionally designed to carry vehicular and pedestrian traffic, transport products, and provide public spaces for social interaction. Paved surfaces also protect underground infrastructure such as waste matter, sewage, electrical wires, and they are further responsible for multiple transport processes of water, matter, and energy between the soil and the atmosphere in urban areas [1]. On the other hand, they have several disadvantages for urban areas, since they lead to an altered hydrological balance compared to rural areas. In 2014, 54% of the world's population lived in urban areas, a proportion that is expected to increase to 66% by 2050 [2]. This increasing urbanization creates many challenges such as flooding [3–6], air pollution [7,8], and altered and heterogeneous microclimates [9,10].

In partly sealed soils, the paving material itself plays the main role in the hydrological balance. The existence of depressions leads to ponding and creates suitable conditions for evaporation [11–14], whereas cracks and slopes alter flow regimes and runoff generation,

respectively [15,16]. Moreover, the construction of the pavers also plays a significant role in the evaporation rate. A study by Starke et al. [17] shows that the sub-base made of a twin-soil layer decreases the evaporation by 16% compared to a homogeneous sub-base.

Applications of lysimeters are the most common methods used to study urban hydrological balance. Few studies provided long-term information on at least two of the three hydrological processes of evaporation, infiltration, and runoff [18–22]. These studies used different types of pavements to cover the lysimeter surfaces (such as asphalt, concrete, cobble-stones, small granite stones, brick pavers).

Timm [22] used Hydro-Pedo-Transfer functions of Wessolek et al. [23] to estimate annual evaporation rates. She applied the equations in two high-resolution weighable lysimeters in Berlin, Germany. These lysimeters are covered in two pavement-sealing types commonly used for sidewalks in Berlin, namely cobble-stones and concrete slabs. The study found that the model offers a good estimation of annual evaporation for cobble-stones and concrete slabs. However, this approach was not designed for estimating monthly or weekly evaporation rates. Until today, there has been no numerical model available for predicting evaporation of sealed areas on a time scale of days or hours.

Different advanced statistical methods have dealt with evaporation and evapotranspiration in urban areas [24–26]. Wang et al. [27] investigated the impact of evapotranspiration (*ET*) on land surface temperature (*LST*) through the modified remote sensing Penman-Monteith (*RS-PM*) model. Vulova et al. [28] used a novel approach to model urban *ET* using remote sensing, flux footprint modeling, and geographic information system (*GIS*) data in addition to deep learning and machine learning techniques. Zeiada et al. [29] used evaporation as one of the quantitative inputs for the machine learning techniques to identify the most sustainable design of asphalt pavement factors prevailing in warm climate regions.

The study used data obtained from paired experiment design using weighable lysimeters under field conditions to determine the mechanism by which two types of soil sealing interact with the same climate conditions in order to explain the differences in evaporation rate above these pavement types. Therefore, we used hourly observations of evaporation from two types of pavements, namely cobble-stones and concrete slabs. All in all, our aims were: (1) to study autocorrelation and partial correlation functions of the evaporation variations from cobble-stones and concrete slabs; (2) to assess temporal patterns between evaporation and covariates from climate drives and soil moisture; and (3) to compare the evaporation rates from cobble-stones and concrete slabs. Ultimately, we want to contribute to a better understanding of evaporation from sealed surfaces in urban areas, considering both meteorological conditions and sealing characteristics.

2. Material and Methods

2.1. Study Area

The study was carried out in the lysimeter station of the German government environmental agency (Umweltbundesamt) located on the southern outskirts of Berlin, Germany (N 52:3967, E 13:3673). The station consists of twelve steel lysimeters and a climate station. Two of the lysimeters are covered by two pavement types: cobble-stones with a large joint area (20%) and concrete slabs (30 × 30 × 4.4 cm) with a narrow joint area (6%) as shown in Figures 1 and 2. The lysimeters have an area of 1 m² and a depth of 50 cm. They consist of (i) a surface layer (4–8 cm) of paving material embedded in fine sand seam material; (ii) construction sand layer beneath; and (iii) gravel and a very coarse sand layer of 10 cm to be used as a drainage layer [19,22]. The lysimeter is weighable and has a resolution of 10 g = 0.01 mm. The covered drain collects runoff and drains it into a weighable tipping bucket based on the device introduced by Nehls et al. [30]. Precipitation (mm), air temperature (°C), wind speed (m s⁻¹), relative humidity (RH) (%), and solar radiation (MJ m⁻²d⁻¹) were measured at the climate station installed next to the lysimeter. Soil moisture was measured at a resolution of 1-minute simultaneously [22]. The data of precipitation, infiltration, evaporation, runoff, and soil moisture from the lysimeter raw data have

been aggregated to a 1-h resolution to obtain the same resolution as the meteorological data. The lysimeter data was processed using the improved adaptive window and adaptive threshold (AWAT) filter routine [31]. AWAT is a moving average and the Savitzky–Golay—filter routine was developed and tested especially for weighting field lysimeter. For more information about the measurement system and the AWAT routine, we refer to Timm [22] and Peters et al. [31].



Figure 1. Lysimeter surfaces: (left), cobble-stones; (right), concrete slabs. Reprinted with permission from Timm [22].

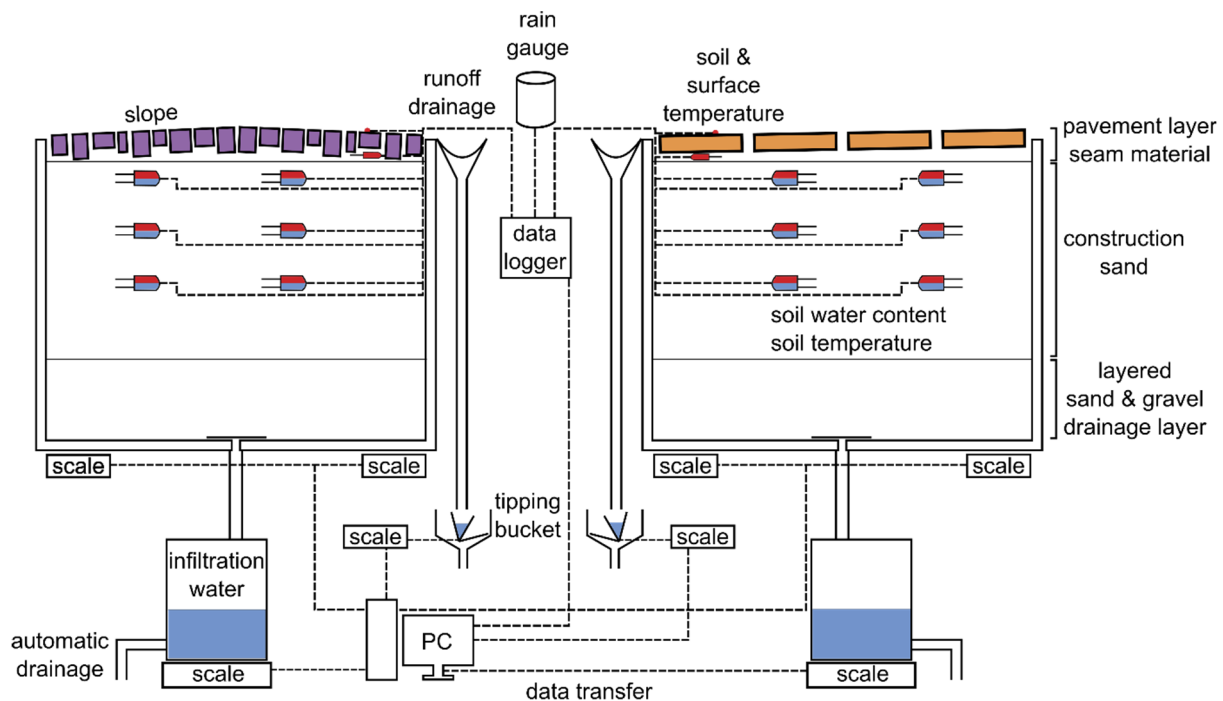


Figure 2. Scheme of lysimeter setup. Reprinted with permission from Timm [22].

2.2. Methodology

2.2.1. Non-Stationarity Process Analysis

Most time series of natural phenomena are non-stationarity. Stationarity is analogous to the concept of an isothermal process within the field of physics. For example, to be able to derive soil physical laws that are deterministic, it is often assumed that the soil

water is isothermal so that energy changes associated with temperature changes do not have to be taken into account. Likewise, in stochastic modeling, the statistical properties of a process are invariant with the time (variance and mean are constant) if the process is stationary. One way to check the non-stationary character of a time series is to look at the autocorrelation function of the series (ACF) and the partial autocorrelation function (PACF). The ACF is the correlation of a variable with itself at differing time lags. PACF checks the correlation at a certain lag after removing the effect of any correlations at shorter lags. When the ACF of the time series converges very slowly, it indicates that the time series is non-stationary.

In this study, we checked the non-stationary structure of the time series of evaporation and its predictors using an autocorrelation function for $24 \text{ h} \times 7 \text{ days}$ (lags). ACF and PACF were carried out in R [32].

2.2.2. Generalized Additive Models (GAMs)

GAMs provide a middle ground between simple models, such as linear regression models, and more complex machine learning models such as neural networks. They can be fitted to complex, nonlinear relationships and produce good predictions, while still being able to produce inferential statistics and understand and explain the underlying model structure. Since most environmental data do not follow a normal distribution, GAMs can find more effective methods to interpret the data than traditional linear models due to their appealing balance between flexibility and interpretability (Wood, 2020).

GAM extends the generalized linear model (GLM) [33] by allowing the predictor function to include nonlinear functions of some or all of the covariates that are not specified a priori [34]. One of the distributions from the exponential family for Y , along with a link function g that relates the expected value of Y to the predictor variables (x) via a structure could be expressed according to wood [35]:

$$g(\mu_i) = X_i^* \theta + f_1(x_{1i}) + f_2(x_{2i}) + f_3(x_{3i}) + \dots \quad (1)$$

where $\mu_i = E(Y_i)$ and Y_i represent some exponential family distributions; f_i are smooth functions; X_i^* is a row of the model matrix for any strictly parametric model components; and θ is the corresponding parameter vector.

Equation (1) shows that the influence of each covariate is captured through a smooth function. The smooth patterns of the covariates can be either linear or non-linear, which provides high flexibility to GAMs. In this study, we used the spline function $s()$ for smoothing the covariates, which can take a wide variety of shapes. We used a tensor function $te()$ to model the interactions that operate on different scales. GAM with a simple smooth model has many coefficients, which is more complex than a linear model where each variable has only a single coefficient.

We fit the GAM to model the urban evaporation using the $bam()$ function from the R package `mgcv` [35]. We wrapped the independent variables (such as meteorological drivers) in the smooth function $s()$ and tensor function $te()$ to specify that the relationship should be flexible. The flexibility could overfit to the data. In fitting a nonlinear model, two aims should be balanced: (i) capturing the relationship by being close to the data; and (ii) avoiding that the model fits the noise. How well GAM captures patterns in the data is measured by likelihood and how much the curve changes shape is measured by the wiggling. The key to a good fit is the trade-off between the two.

Applying interactions between predictors refers to a key to the correct interpretation of data. Interactions in models represent the fact that outcomes depend on non-independent relationships of multiple variables. In a GAM, the relationship between a variable and an outcome changes across the range of the smooth. Similarly, interactions are different across all of the values of two or more variables. In this study, we captured the non-stationary and temporal patterns of evaporation and its drivers of the data by adding the time predictor in the form of days as an independent variable using smooth function $s()$ and in the form of hours when it interacts with meteorological data using tensor function $te()$ which enables

the interactions with different scales (in our case: time with solar radiation, time with relative humidity and time with wind speed).

GAMs are built using evaporation (log scale) as a response variable and the following predictors as explanatory variables: precipitation accumulated over 10 h, relative humidity, air temperature, solar radiation, wind speed at 10 m, runoff, and infiltration. In this study, the response variable (evaporation) and predictors (climate and soil data) did not change at a constant rate over time (non-stationary, see Supplementary Materials. Thus, time was added as an interactions predictor to the model to control for seasonal and other temporal trends [36]. Three models were built to assess the evaporation variation: first one for the evaporation from cobble-stone, second one for the evaporation from concrete slabs, and third one for the difference in evaporation between cobble-stones and concrete slabs.

GAM for cobble-stones

$$bam(\log(Evaporation)) \sim S(Day, k = 100) + S(runoff) + s(infiltration) + S(10h, rainfall_{accumulation}, K = 5) + te(Hour, soil\ radiation) + te(Hour, relative\ humidity) + te(Hour, wind\ speed_{10cm}), data = data, method = "REML" \quad (2)$$

GAM for concrete slabs

$$bam(\log(Evaporation)) \sim S(Day, k = 100) + S(runoff, k = 4) + s(infiltration, K = 3) + te(Hour, solar\ radiation) + te(Hour, relative\ humidity) + (10h, rainfall_{accumulation}, air\ temperature), data = data, method = "REML" \quad (3)$$

GAM for the difference in evaporation between cobble-stones and concrete slabs

$$bam(evaporation_{cobble\ stones} - evaporation_{concrete\ slabs}) \sim s(Day, k = 100) + S(10h, rainfall_{accumulation}, k = 5) + te(Hour, solar\ radiation) + te(Hour, relative\ humidity) + te(Hour, wind\ speed_{10cm}) \quad (4)$$

K in the models represent a number of basis function that affects how wiggly GAM function can be.

The evaporation data are asymmetric. Most values are close to zero and do not have a normal distribution. Thus, we transformed them by adding a constant and used logarithm values in order to make the distributions more symmetric (Gaussian family). Visual inspection of the residual plots did not reveal any major deviations from homoscedasticity or normality. Specifically, the evaporation was log-transformed to meet the demand for residual normality and homoscedasticity. *p* values were used to determine which nonlinear relationships in the model and which explanatory variables should be excluded from the model. We chose the model when the lower Akaike information criterion (AIC) was obtained with significant explanatory variables [37].

The two lysimeters being located close to each other enables us to use the paired experiment design to compare evaporation from the two sealing soils, where the two pavement types undergo the same climatic conditions. Although the climate factors are not controlled, this design enables us to confirm that the main difference in evaporation rate from these sealing soils is due to the soil-atmosphere interface type.

3. Results

In the evaporation process from the soil surface, solar radiation and air temperature change the state of water molecules from liquid to vapor. The difference between the water vapor pressure at the evaporating surface and that of the surrounding atmosphere is the main factor driving the removal of water vapor from the evaporating surface. As the surrounding air becomes saturated, the evaporation process slows down and may even stop if the air is not transferred to the atmosphere. The replacement of saturated air with drier air depends mostly on wind speed. Hence, solar radiation, air temperature, air humidity, and wind speed are the main climatological drivers that should be considered when evaluating evaporation [38]. Moreover, Where the evaporating surface is the soil

surface, water from a shallow water table is transported upwards in the soil to moisten the soil surface. In such soil, water is supplied quickly enough to meet the evaporation demand. In this study, we investigate the changes in the evaporation process as described above when the soil surface is paved.

Below we will describe, aggregate, and present the significant relationship between the collected data. These data could help to understand the patterns of evaporation in urban soils where the evaporating surfaces are cobble-stones and concrete slabs. Then, we will investigate temporal trends, variability, and interactions between evaporation and its environmental drivers and assess the variation of evaporation from cobble-stones and concrete slabs by building a generalized additive model (GAM) for each pavement type.

3.1. Descriptive Analyses of the Evaporation and Its Drivers

The amount of precipitation is important to the overall hydrological cycle. Table 1 shows a good correlation between precipitation accumulated over 10 h and evaporation from the two pavements. Depending on the properties of the pavement, annual and seasonal hydrological processes react differently. Figure 3 illustrates the hydrological balances of two pavements with detailed values in Table 2. Although infiltration is almost the same for both surfaces, the annual and seasonal (summer and winter) values are higher than evaporation and runoff.

Table 1. Correlation between the precipitation accumulated over 10 h and evaporation from the two pavements.

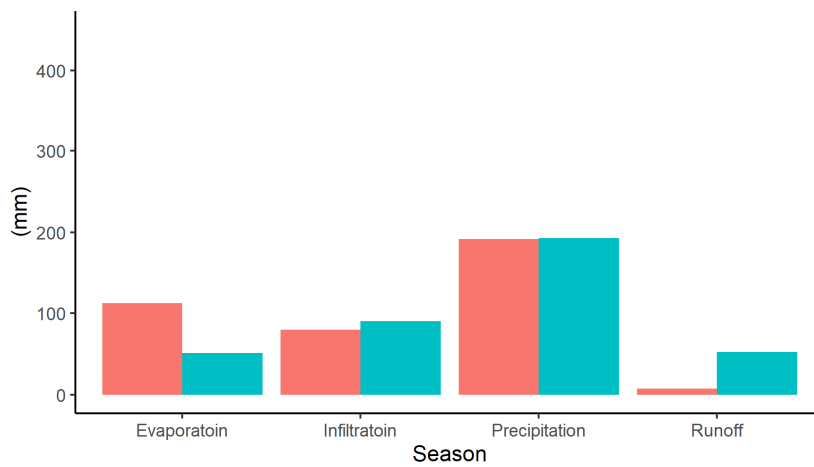
	Accumulation of Precipitation over 10 h									
	1 h	2 h	3 h	4 h	5 h	6 h	7 h	8 h	9 h	10 h
Evaporation from cobble stone	0.01	0.01	0.10	0.17	0.21	0.26	0.32	0.37	0.41	0.43
Evaporation from concrete slabs	0.01	0.06	0.15	0.20	0.24	0.26	0.26	0.26	0.27	0.28

Table 2. Hydrological data balance (June 2016 to June 2017, annual, summer, winter) with absolute (mm) value and share (%).

	Cobble-Stones				Concrete Slabs			
	Precipitation mm	Infiltration mm (%)	Runoff mm (%)	Evaporation mm (%)	Precipitation mm	Infiltration mm (%)	Runoff mm (%)	Evaporation mm (%)
Annual	414.51	257.07 (62.2)	10.74 (2.5)	156.82 (34.5)	422.72	261.88 (61.9)	74.8 (17.6)	93.92 (22.21)
Summer	192.29	79.89 (42.54)	7.58 (3.9)	112.07 (58.28)	193.01	90.03 (46.64)	52.21 (27.03)	51.18 (26.5)
Winter	222.22	177.18 (79)	3.16 (1.4)	44.75 (20.13)	229.71	171.45 (74.63)	22.59 (9.83)	42.74 (18.6)

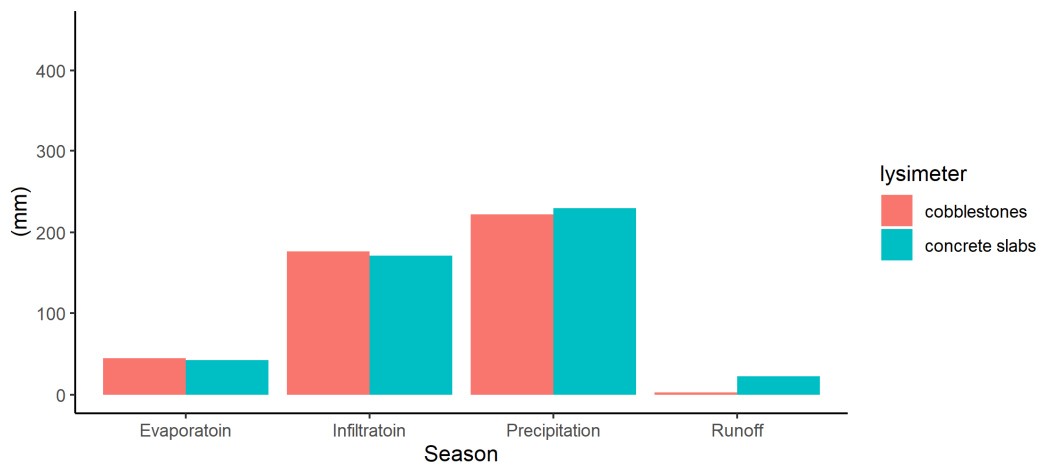
Summer

Hydrological balance of Cobblestones and concrete slabs
June 2016 to June 2017.



Winter

Hydrological balance of Cobblestones and concrete slabs
June 2016 to June 2017.



Annual

Hydrological balance of Cobblestones and concrete slabs
June 2016 to June 2017.

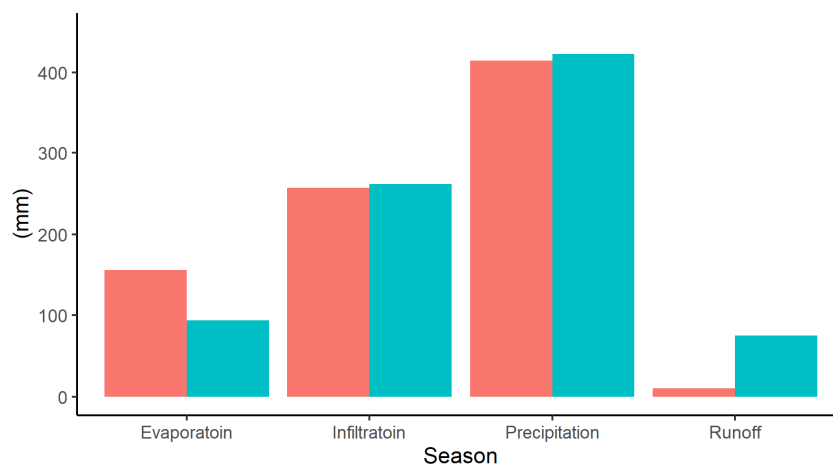


Figure 3. One-year (June 2016 to June 2017) measured hydrological balance of paved surfaces in Berlin, Germany, summer—May to October, and winter—November to April (mm).

Evaporation and runoff differ significantly between the two pavement types. Cobblestones evaporate twice as much as concrete slabs during the summer, while concrete slabs generate runoff almost seven times higher than cobblestones (Figure 3). In winter, both surfaces evaporate the same amount of water. In summer, cobblestones evaporate twice as much as concrete slabs (Table 2). Median daily of evaporation from cobblestones for each month shows higher value in summer than in winter. For concrete slabs, median daily of evaporation has no clear pattern during the year (Figure S1)

Moreover, values of soil moisture at 5 cm below the underside of the paver are significantly different and they are considered as another evidence that the characteristics of these two pavement types altered hydrological balance differently (Figure 4). Focusing on the evaporation, properties of the pavement also affect the patterns of evaporation diurnally and seasonally. Since the interface between cobblestones and the atmosphere has a good connection with the soil (more than 20% seam), solar radiation has somehow a similar effect on the evaporation rate from cobblestones as from natural soil surfaces (Figure 5), where the evaporation rate is significantly higher during the day than at night. Figure 5 also shows that the concrete evaporation's values at night are somehow equal to its values at daytime. Due to the thermal diffusivity of the pavements and their structure, the surface of the pavements absorbs heat and transmits it to the lower structural layers through heat conduction in the daytime. At night, heat is transferred to the upper part of the concrete [39], leading to a significant role in the evaporation process at night. These results were also confirmed by Cao et al. [40], who found that large amounts of solar radiation are absorbed by pavements during the day and released during the nighttime.

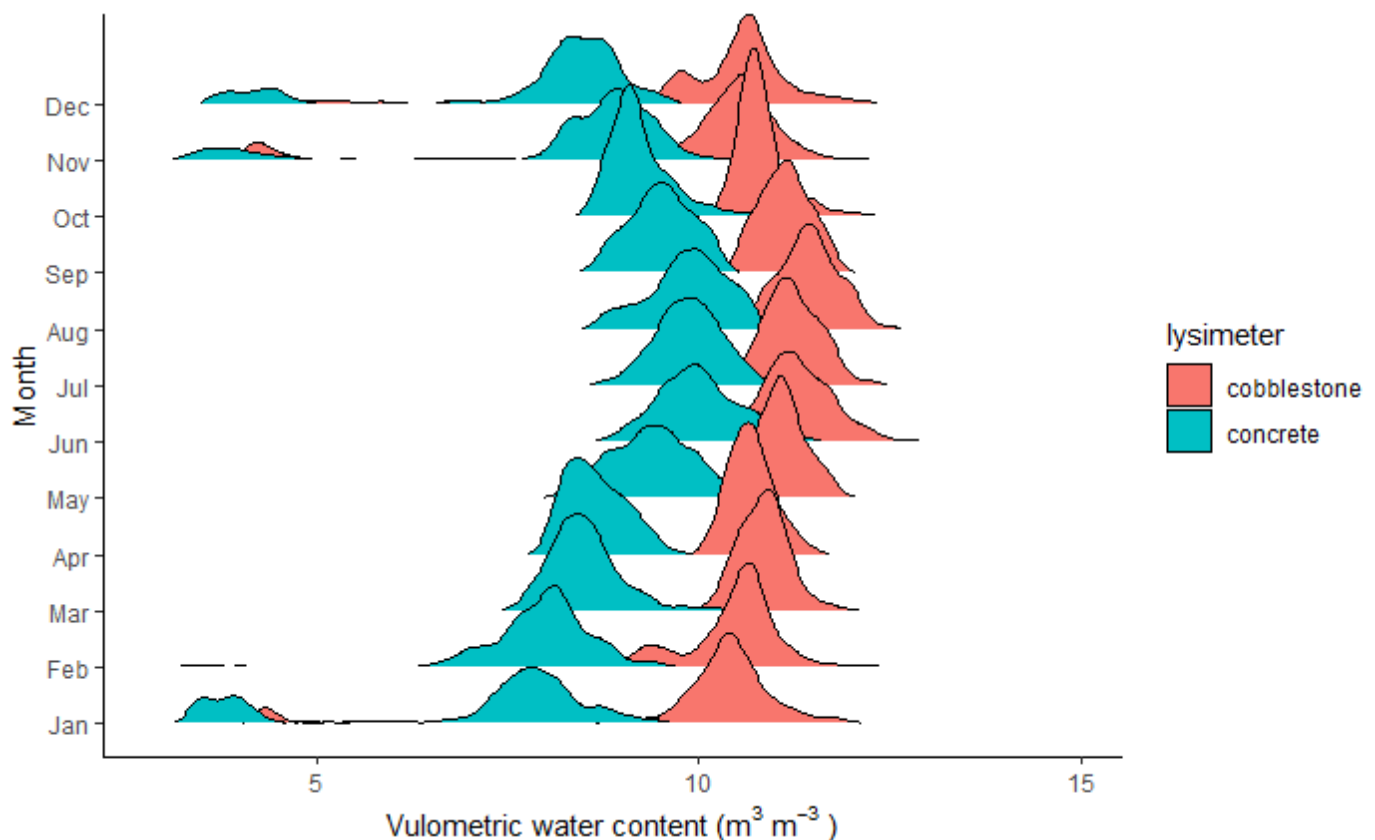


Figure 4. Distribution of soil moisture 5 cm beneath cobble stones and concrete slabs.

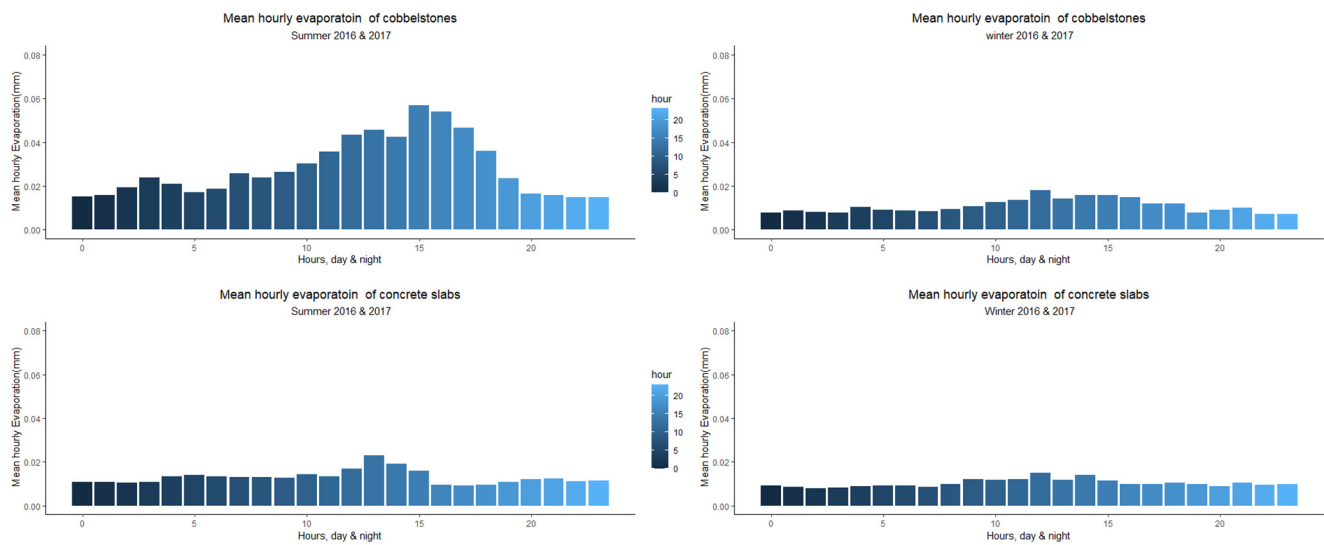


Figure 5. Mean measured hourly evaporation during day- and night-time from cobble stones and concrete slabs during summer (May to October), and winter time (November to April), mm.

3.2. Temporal Trends, Variability, and Interactions between Evaporation and Its Environmental Drivers

In this study, since evaporation time series and its environmental drivers are observed at a high temporal resolution, the autocorrelation of datasets and their temporal variability are critical for understanding processes and their interactions. Figure 6 shows the autocorrelation function (ACF) of the evaporation time series of cobble-stones and concrete slabs. The ACF converges very slowly indicating non-stationary time series [41]. The four primary meteorological time series drivers of evaporation (solar radiation, wind speed, atmospheric humidity, and air temperature) are also non-stationary times series with significant autocorrelation structures. The ACF confirms the seasonality every 24 h (Figure S2). Figure S3 shows clear seasonal patterns (day and night) of meteorological drivers by depicting its hourly boxplot.

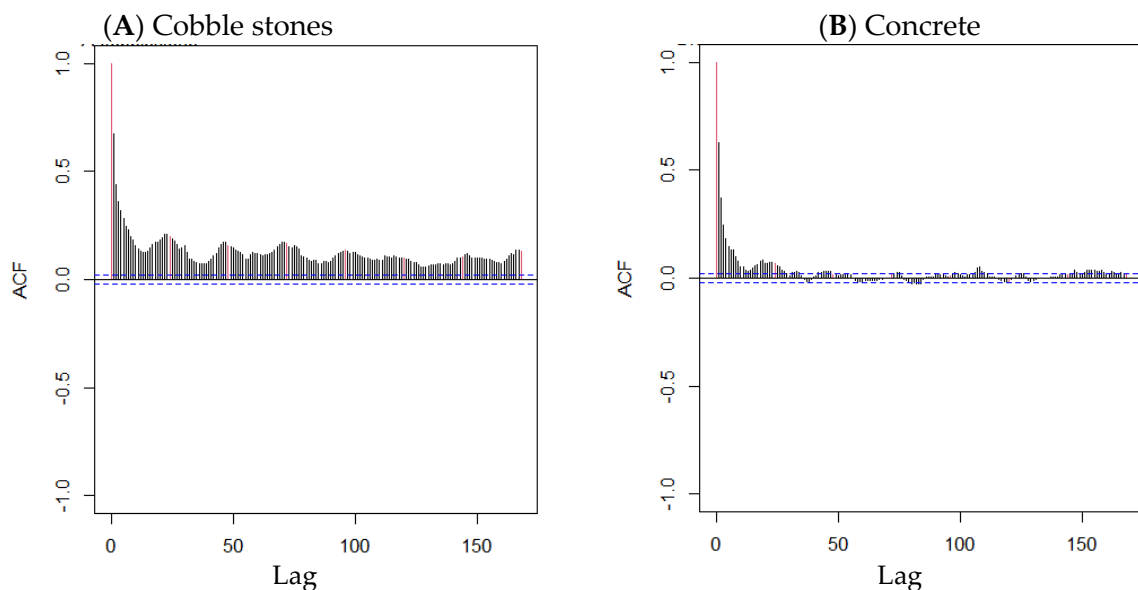


Figure 6. Autocorrelation function (ACF) for time series evaporation. (A) ACF for cobble-stones, (B) ACF for concrete. The ACF of the original data indicates that the series is not stationary. The dotted line is $2 \times$ standard errors.

3.3. Generalized Additive Model

To evaluate the variation of evaporation from cobble-stones and concrete slabs, we built GAM where the evaporation is the response variable and its traditional predictors are the four meteorological drivers (solar radiation, relative humidity, air temperature, and wind speed) [38]. Moreover, based on the information shown in Figures 3 and 6, more predictors could be added to explain the variation of urban evaporation. First, the time is added as an explanatory variable; as shown in Figure 6, there are strong dependencies between smaller lags. Figure 6 shows the ACF plot for $k = 168$, with the Y-axis having correlation (r) values ranging between 0 and 1. With $k = 1$ having $r > 0.60$ for cobble-stones and concrete slabs. Moreover, the time variable interacts with the meteorological drivers to account for the temporal pattern of evaporation and its associated affecting factors. Second, the model also included the runoff and infiltration values. Figure 3 showed that runoff is significantly higher from concrete slabs than cobble-stones and infiltrations values differ from winter to summer for each paver.

After running the model (2) and (3), Figure 7 shows the result of evaporation response to its predictors.

Runoff: The type of upper layers of paver and seam material absorbing and detaining water (surface wetting) could explain the relationship between runoff and evaporation. Once this layer is saturated, the runoff will begin to flow towards local depressions, where part of the water will be lost to infiltration and evaporation. Runoff from concrete slabs is nearly seven times that of cobble-stones (Figure 3). Figure 7 shows that the evaporation from concrete slabs becomes lower than its means as the runoff increases depicting a nonlinear relationship pattern. While the runoff was not a significant variable and is excluded to explain the variation of evaporation from cobble-stones in the model (2).

Infiltration: Both surfaces led to similar infiltration, but the infiltration in winter for both surfaces is nearly double its values in summer. In contrast, the evaporation values in summer are higher than in winter for both surfaces (Figure 3). The difference in precipitation patterns could explain this increase of runoff and evaporation and decrease of infiltration from winter to summer [22]. GAM models (2) and (3) show that the evaporation values of pavements decrease nonlinearly as the infiltration increases. The evaporation's value decreases below its mean when infiltration's value > 0.5 mm and > 3.2 mm for concrete slabs and cobble-stones, respectively (Figure 7). This could be explained due to the seam material shared on both surfaces, where the seam in cobble-stones retains the water during the infiltration and evaporates later.

Solar radiation: Little variation of evaporation is observed above concrete slabs between day and night, while evaporation from cobble-stones showed clear variations between day and night (Figure 5). The results of the solar radiation as an explanatory variable obtained from the model (2) and (3) for cobble-stones and concrete slabs confirmed what is observed in Figure 5. Due to the thermal diffusivity of the pavements and their structure, the surface of the pavements absorbs heat and transmits it to the lower structural layers through heat conduction in the daytime. At night, heat is transferred to the upper part of the concrete [39], leading to a significant role in the evaporation process at night. Figure 7 showed this information by solar radiation. For cobble-stone, Figure 7 from model (2) shows that in the daytime there is higher evaporation with higher solar radiation and the evaporation continues during the night. As previously mentioned, the solar radiation effect on evaporation from cobble-stones with a large joint area (20%) has almost a similar pattern on the evaporation rate as from natural soil surfaces during the daytime, while the evaporation during the nighttime is due to the absorbed solar radiation during the daytime and released it during the nighttime. For concrete slabs with just 6% of a joint area, released solar radiation during the nighttime is clear. These results were also confirmed by Cao et al. [40], who found that large amounts of solar radiation are absorbed by pavements during the day and released during the nighttime. With high solar radiation (more than $500 \text{ MJ m}^{-2} \text{ d}^{-1}$) at daytime, the expected change in evaporation by GAM increases by 27

and 20% for cobble-stones and concrete slabs, respectively, the prediction occurred not only during the day but also at nighttime.

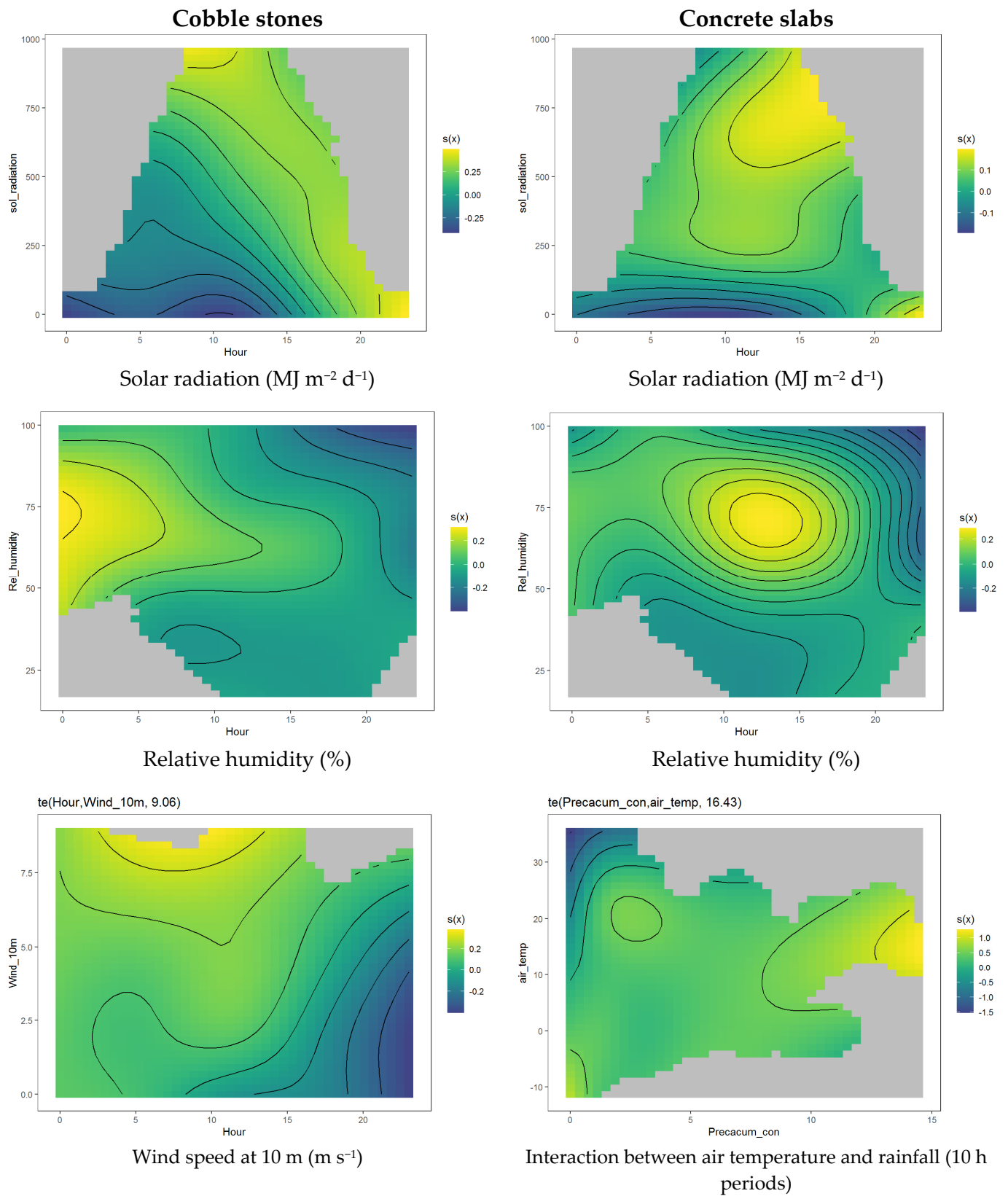


Figure 7. Cont.

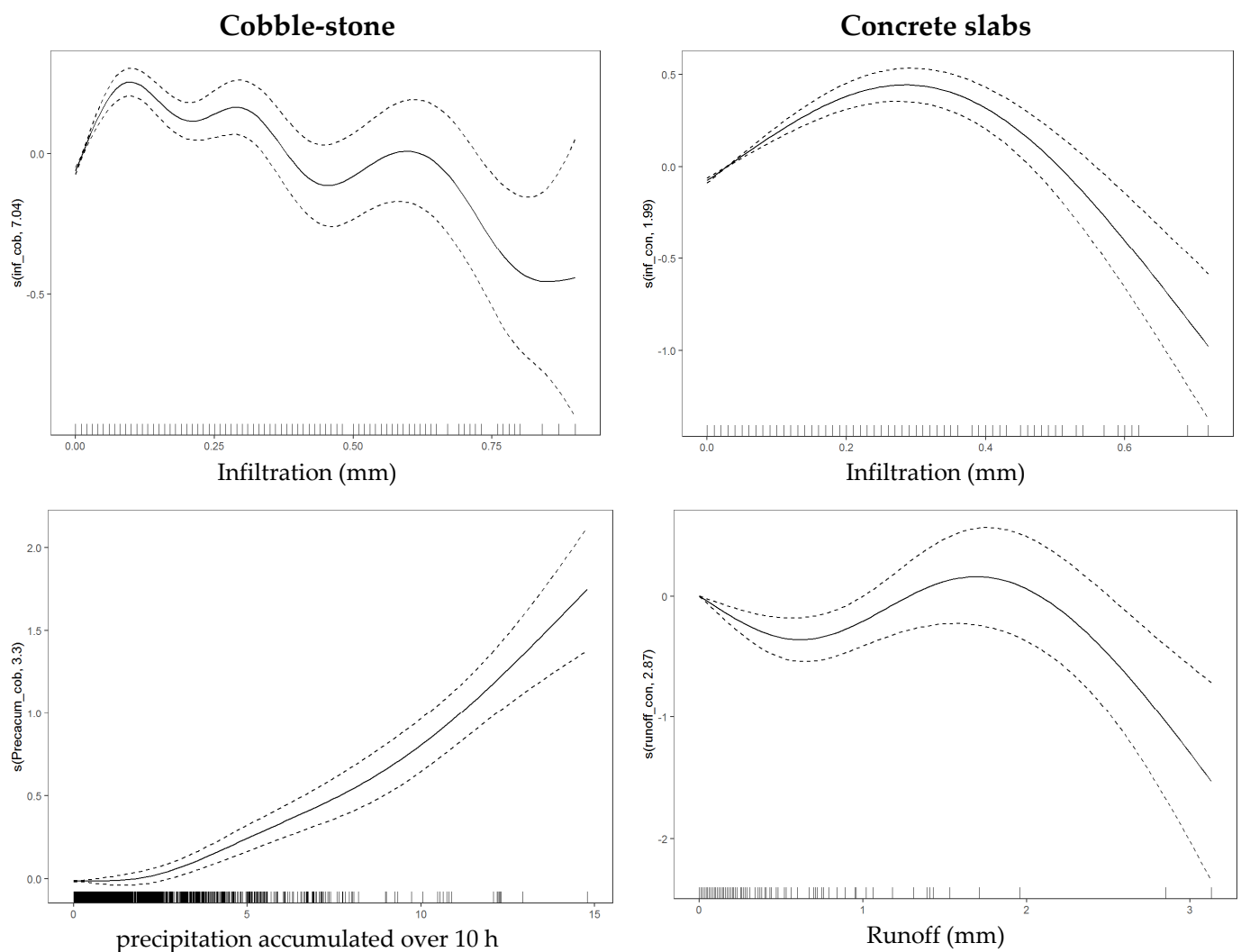


Figure 7. Explanatory variables that explain the variation of evaporation above cobble-stones and concrete slabs surfaces used in GAM model (2 and 3).

Accumulation of precipitation: GAM model (2) shows that the amount of accumulated precipitation has a positive nonlinear relationship with evaporation from cobble-stones (Figure 7). Again, this could illustrate the seam material retains the water and evaporates later [16]. The GAMs predict a 33% expected change in evaporation increase from cobble-stones surface associated with the 5 mm of total precipitation accumulated over 10 h.

Relative humidity: Figure 7 shows that the concrete slabs produce high values of evaporation during the daytime when relative humidity is within the range of 50% to 80%, cobble-stones have high evaporation values during the nighttime when relative humidity ranges between 50% and 85%. This result could be explained since when relative humidity is $>80\%$ the evaporation process from pavements will slow down and might stop if the wet air is not transferred to the atmosphere. Figure 7 shows also that during the daytime, the evaporation from concrete slabs is high with higher relative humidity and the evaporation from cobble-stone is high with higher solar radiation. With high relative humidity (more than 60%) at nighttime, the expected change in evaporation by GAM model (2) increases by 21% for cobble-stones, and the expected change in evaporation from concrete slabs model (3) increases almost in the same value but when the relative humidity more than 60% during the daytime.

As we mentioned above, from Figure 7, looking at the effect of relative humidity (between 50% and 80%) on the evaporation from cobble-stone we see that the evaporation

produces a higher quantity at nighttime (unit almost 5 am) where there is no solar radiation, now to understand well these findings we have to look on the plot below where we could see the effect of another explanatory variable on the evaporation (wind speed). We can see this higher quantity of evaporation at nighttime due to high wind speed. Moreover, in concrete slabs lysimeter, we see that the maximum evaporation rate produced when the relative humidity ranged between 50% and 80%, but the time is between 8 am and 16 pm where there is higher solar radiation. As a result, at the same level of relative humidity, cobble-stone is more sensitive to producing evaporation at nighttime when there is an increase in wind speed. On the other hand, in concrete slabs the solar radiation dominates the evaporation process during the daytime.

Wind speed and soil temperature: Wind speed is included in model (2) as a significant variable to explain the variation of evaporation values from cobble-stones. According to model (2) (Figure 7), wind speed's values higher than 7.5 m s^{-1} could explain the high evaporation value in the morning, GAM model (2) predict a 21% expected change in evaporation increase from cobble-stone surface. When the air temperature is higher than $10 \text{ }^\circ\text{C}$ and the precipitation accumulated over 10 h higher than 12 mm, GAM model (3) predicts more than 33% expected change in evaporation increase from concrete slabs surface.

Moreover, a new GAM is built where its response variable is the difference between evaporation from cobble stones and the evaporation from concrete slabs and the explanatory variables are the climate drivers. Model (4) shows the significant explanatory climate drivers that could explain the differences in evaporation between the two pavement types.

Figure 8 shows that under the same climatic conditions, cobble stones more prone to increasing the evaporation rate than concrete slabs when the precipitation accumulated over 10 hours, solar radiation and wind speed increases. While concrete slabs more inclined to increase the evaporation rate than cobble stones when the relative humidity increases.

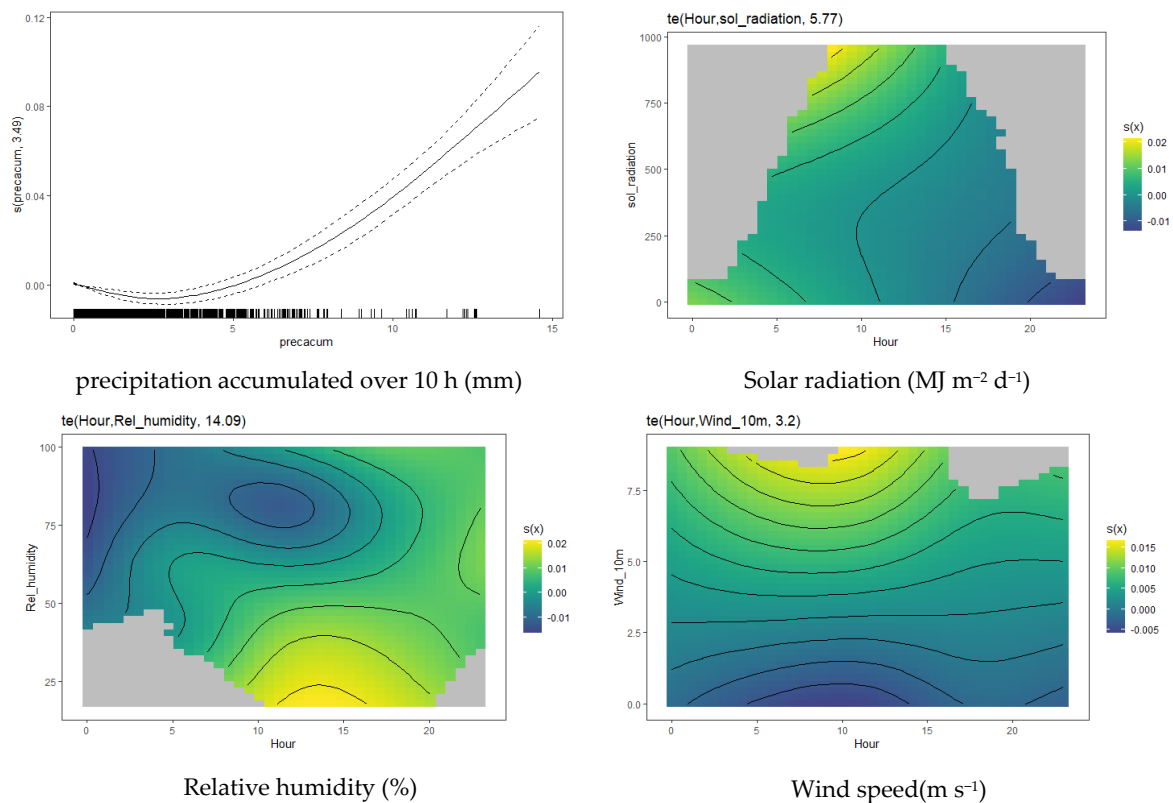


Figure 8. Explanatory variables that explain the difference of evaporation between cobble-stones and concrete slabs surfaces used in GAM (model 4).

4. Conclusions

This study used a unique dataset to gain new insights into the urban hydrological balance (and in particular, to understand and explain how two different soil sealing types affect evaporation rates under the same climatic conditions). Hourly time series of evaporation, runoff, and infiltration were obtained from two high-resolution weighable lysimeters covered in two pavement-sealing types commonly used for sidewalks in Berlin, Germany: cobble-stones and concrete slabs. Soil volumetric water was observed in the lysimeters with capacitance soil moisture sensors at 5 cm depth. Moreover, time series consisting of hourly climatological measurements were observed by a climate station located near the lysimeters.

Matching pairs is a powerful experimental designed to compare the evaporation above two soil sealing under the same climatic conditions. Generalized additive models (GAMs) are able to visualize and explain each climatic driver's effect on the variation of evaporation and how its effect changes when the sealing type changes. Using GAMs to compare evaporation from two sealing soil types under the same climatic conditions, cobble-stones are more likely to increase the rate of evaporation than concrete slabs when the precipitation accumulated over 10 h, solar radiation, and wind speed increases. In contrast, concrete slabs are more prone to increase the rate of evaporation than cobbles-tones when the relative humidity increases. GAMs are a powerful tool to explain the interaction between climatic conditions and evaporation rate and to show the mechanism by how soil sealing type affects evaporation rate under the same climatic conditions.

Supplementary Materials: The following supporting information can be downloaded at: <https://www.mdpi.com/article/10.3390/land11040508/s1>, Figure S1: Daily evaporation by month for cobble stones and concrete slabs; Figure S2: Autocorrelation function (ACF) for time series; Figure S3: Hourly box plot of meteorological variables as measured June 2016 to June 2017 in Berlin.

Author Contributions: Conceptualization, B.A. and J.A.S.-E.; Methodology, B.A. and J.A.S.-E.; software, J.A.S.-E. and B.A.; validation, J.A.S.-E. and B.A.; formal analysis, B.A. and J.A.S.-E.; investigation, B.A., J.A.S.-E., G.W. and B.K. (Björn Kluge); resources, B.K. (Björn Kluge), G.W. and B.A.; data curation, B.K. (Björn Kluge), G.W. and B.A.; writing—original, B.A., J.A.S.-E. and G.W.; draft preparation, B.A. and G.W.; writing—review and editing, B.A., J.A.S.-E., B.K. (Björn Kluge), B.K. (Birgit Kleinschmit) and G.W.; visualization, B.A., G.W. and J.A.S.-E.; supervision, G.W. and B.K. (Birgit Kleinschmit); project administration, B.K. (Birgit Kleinschmit). All authors have read and agreed to the published version of the manuscript.

Funding: The German Research Foundation DFG (GRK 2032) and the Open Access Publication Fund of TU Berlin.

Institutional Review Board Statement: Not applicable.

Informed Consent Statement: Not applicable.

Data Availability Statement: The data presented in this study are available on reasonable request from the corresponding author.

Acknowledgments: We would like to thank the German Research Foundation DFG (GRK 2032) and the Open Access Publication Fund of TU Berlin for funding this study as part of the 'Urban Water Interfaces' research-training group. We are grateful to Anne Timm for collecting, cleaning, and organizing the data and to Stenka Vulova for language editing the manuscript.

Conflicts of Interest: The authors declare no conflict of interest.

References

1. Dong, J.; Meng, W.; Liu, Y.; Ti, J. A framework of pavement management system based on IoT and big data. *Adv. Eng. Inform.* **2021**, *47*, 101226. [[CrossRef](#)]
2. Crocker-Buque, T.; Mindra, G.; Duncan, R.; Mounier-Jack, S. Immunization, urbanization and slums — A systematic review of factors and interventions. *BMC Public Health* **2017**, *17*, 556. [[CrossRef](#)] [[PubMed](#)]
3. Haase, D. Effects of urbanisation on the water balance—A long-term trajectory. *Environ. Impact Assess. Rev.* **2009**, *29*, 211–219. [[CrossRef](#)]

4. Pistocchi, A.; Calzolari, C.; Malucelli, F.; Ungaro, F. Soil sealing and flood risks in the plains of Emilia-Romagna, Italy. *J. Hydrol. Reg. Stud.* **2015**, *4*, 398–409. [CrossRef]
5. Qin, H.-P.; Li, Z.-X.; Fu, G. The effects of low impact development on urban flooding under different rainfall characteristics. *J. Environ. Manag.* **2013**, *129*, 577–585. [CrossRef] [PubMed]
6. Bayazit, Y.; Koç, C.; Bakış, R. Urbanization impacts on flash urban floods in Bodrum Province, Turkey. *Hydrol. Sci. J.* **2021**, *66*, 118–133. Available online: <https://www.tandfonline.com/doi/abs/10.1080/02626667.2020.1851031> (accessed on 18 March 2022). [CrossRef]
7. Rodríguez, M.C.; Dupont-Courtade, L.; Oueslati, W. Air pollution and urban structure linkages: Evidence from European cities. *Renew. Sustain. Energy Rev.* **2016**, *53*, 1–9. [CrossRef]
8. Rahman, M.M.; Alam, K. Clean energy, population density, urbanization and environmental pollution nexus: Evidence from Bangladesh. *Renew. Energy* **2021**, *172*, 1063–1072. [CrossRef]
9. Chatzidimitriou, A.; Yannas, S. Microclimate development in open urban spaces: The influence of form and materials. *Energy Build.* **2015**, *108*, 156–174. [CrossRef]
10. Kwok, Y.T.; Schoetter, R.; de Munck, C.; Lau, K.K.-L.; Wong, M.S.; Ng, E. High-resolution mesoscale simulation of the microclimatic effects of urban development in the past, present, and future Hong Kong. *Urban Clim.* **2021**, *37*, 100850. [CrossRef]
11. Mansell, M.; Rollet, F. The effect of surface texture on evaporation, infiltration and storage properties of paved surfaces. *Water Sci. Technol.* **2009**, *60*, 71–76. [CrossRef] [PubMed]
12. Nehls, T.; Menzel, M.; Wessolek, G. Depression storage capacities of different ideal pavements as quantified by a terrestrial laser scanning-based method. *Water Sci. Technol.* **2015**, *71*, 862–869. [CrossRef] [PubMed]
13. Nehls, T.; Peters, A.; Kraus, F.; Rim, Y.N. Water dynamics at the urban soil-atmosphere interface—rainwater storage in paved surfaces and its dependence on rain event characteristics. *J. Soils Sediments* **2021**, *21*, 2025–2034. [CrossRef]
14. Jin, L.; Yang, B.; Yuan, S. Investigation of Evaporation and Cracking of Soil Reinforced with Natural and Polypropylene Fibers. *J. Nat. Fibers* **2021**, 1–15. [CrossRef]
15. Hibbs, B.J.; Sharp, J.M., Jr. Hydrogeological Impacts of Urbanization. *Environ. Eng. Geosci.* **2012**, *18*, 3–24. [CrossRef]
16. Starke, P.; Göbel, P.; Coldewey, W.G. Urban evaporation rates for water-permeable pavements. *Water Sci. Technol.* **2010**, *62*, 1161–1169. [CrossRef] [PubMed]
17. Starke, P.; Göbel, P.; Coldewey, W.G. Effects on evaporation rates from different water-permeable pavement designs. *Water Sci. Technol.* **2011**, *63*, 2619–2627. [CrossRef] [PubMed]
18. Flöter, O. Wasserhaushalt Gepflasterter Straßen und Gehwege: Lysimeterversuche an Drei Aufbauten Unter Praxisnahen Bedingungen Unter Hamburger Klima. Ph.D. Thesis, Verein zur Förderung der Bodenkunde in Hamburg, Hamburg, Germany, 2006.
19. Rim, Y.-N. Analyzing Runoff Dynamics of Paved Soil Surface Using Weighable Lysimeters. Ph.D. Thesis, Technische Universität Berlin, Berlin, Germany, 2011.
20. Ragab, R.; Rosier, P.; Dixon, A.; Bromley, J.; Cooper, J.D. Experimental study of water fluxes in a residential area: Road infiltration, runoff and evaporation. *Hydrol. Process.* **2003**, *17*, 2423–2437. [CrossRef]
21. Xiang, W.; Si, B.; Li, M.; Li, H.; Lu, Y.; Zhao, M.; Feng, H. Stable isotopes of deep soil water retain long-term evaporation loss on China's Loess Plateau. *Sci. Total Environ.* **2021**, *784*, 147153. [CrossRef] [PubMed]
22. Timm, A. Water and Heat Transport of Paved Surfaces. Ph.D. Thesis, Technische Universität Berlin, Berlin, Germany, 2019. [CrossRef]
23. Wessolek, G.; Duijnsveld, W.; Trinks, S. Hydro-pedotransfer functions (HPTFs) for predicting annual percolation rate on a regional scale. *J. Hydrol.* **2008**, *356*, 17–27. [CrossRef]
24. Yamagata, H.; Nasu, M.; Yoshizawa, M.; Miyamoto, A.; Minamiyama, M. Heat island mitigation using water retentive pavement sprinkled with reclaimed wastewater. *Water Sci. Technol.* **2008**, *57*, 763–771. [CrossRef] [PubMed]
25. Nouri, H.; Nagler, P.; Borujeni, S.C.; Munez, A.B.; Alaghmand, S.; Noori, B.; Galindo, A.; Didan, K. Effect of spatial resolution of satellite images on estimating the greenness and evapotranspiration of urban green spaces. *Hydrol. Processes* **2020**, *34*, 3183–3199. [CrossRef]
26. Nouri, H.; Beecham, S.; Kazemi, F.; Hassanli, A.M. A review of ET measurement techniques for estimating the water requirements of urban landscape vegetation. *Urban Water J.* **2013**, *10*, 247–259. [CrossRef]
27. Wang, Y.; Zhang, Y.; Ding, N.; Qin, K.; Yang, X. Simulating the Impact of Urban Surface Evapotranspiration on the Urban Heat Island Effect Using the Modified RS-PM Model: A Case Study of Xuzhou, China. *Remote Sens.* **2020**, *12*, 578. [CrossRef]
28. Vulova, S.; Meier, F.; Rocha, A.D.; Quanz, J.; Nouri, H.; Kleinschmit, B. Modeling urban evapotranspiration using remote sensing, flux footprints, and artificial intelligence. *Sci. Total Environ.* **2021**, *786*, 147293. [CrossRef] [PubMed]
29. Zeiada, W.; Abu Dabous, S.; Hamad, K.; Al-Ruzouq, R.; Khalil, M.A. Machine Learning for Pavement Performance Modelling in Warm Climate Regions. *Arab. J. Sci. Eng.* **2020**, *45*, 4091–4109. [CrossRef]
30. Nehls, T.; Rim, Y.N.; Wessolek, G. Technical note on measuring run-off dynamics from pavements using a new device: The weighable tipping bucket. *Hydrol. Earth Syst. Sci.* **2011**, *15*, 1379–1386. [CrossRef]
31. Peters, A.; Nehls, T.; Wessolek, G. Technical note: Improving the AWAT filter with interpolation schemes for advanced processing of high resolution data. *Hydrol. Earth Syst. Sci.* **2016**, *20*, 2309–2315. [CrossRef]
32. RC Team. *R: A Language and Environment for Statistical Computing*; R Foundation for Statistical Computing: Vienna, Austria, 2013.

33. Hastie, T.; Tibshirani, R. Generalized Additive Models: Some Applications. *J. Am. Stat. Assoc.* **1987**, *82*, 371. [[CrossRef](#)]
34. Polansky, L.; Robbins, M.M. Generalized additive mixed models for disentangling long-term trends, local anomalies, and seasonality in fruit tree phenology. *Ecol. Evol.* **2013**, *3*, 3141–3151. [[CrossRef](#)] [[PubMed](#)]
35. Wood, S.N. *Generalized Additive Models: An Introduction with R*; CRC Press: Boca Raton, FL, USA, 2017.
36. Ramsay, T.O.; Burnett, R.T.; Krewski, D. The Effect of Concurvity in Generalized Additive Models Linking Mortality to Ambient Particulate Matter. *Epidemiology* **2003**, *14*, 18–23. [[CrossRef](#)] [[PubMed](#)]
37. Burnham, K.P.; Anderson, D.R. Multimodel inference: Understanding AIC and BIC in model selection. *Sociol. Methods Res.* **2004**, *33*, 261–304. [[CrossRef](#)]
38. Allen, R.G.; Pereira, L.S.; Raes, D.; Smith, M. Crop evapotranspiration—Guidelines for computing crop water requirements—FAO Irrigation and drainage paper. *FAO Rome* **1998**, *300*, D05109.
39. Yang, H.; Yang, K.; Miao, Y.; Wang, L.; Ye, C. Comparison of Potential Contribution of Typical Pavement Materials to Heat Island Effect. *Sustainability* **2020**, *12*, 4752. [[CrossRef](#)]
40. Cao, X.J.; Tang, B.M.; Zou, X.L.; He, L.H. Analysis on the cooling effect of a heat-reflective coating for asphalt pavement. *Road Mater. Pavement Des.* **2015**, *16*, 716–726. [[CrossRef](#)]
41. Brocklebank, J.C.; Dickey, D.A. *SAS for Forecasting Time Series*; John Wiley & Sons: Hoboken, NJ, USA, 2003.